

# Advanced modeling tools for laser-plasma accelerators (LPAs)

## 3/3

Carlo Benedetti  
LBNL, Berkeley, CA, USA  
(with contributions from R. Lehe, J.-L. Vay, T. Mehrling)



Advanced Summer School on

*“Laser-Driven Sources of High Energy Particles and Radiation”*

9-16 July 2017, CNR Conference Centre,  
Anacapri, Capri, Italy

# Overview of lecture 3

- Modeling of LPAs using tools beyond standard PIC (computational gains and limitations):
  - Lorentz boosted frame;
  - Laser-envelope description (i.e., ponderomotive guiding center);
  - Quasi-static approximation;
  - Quasi-cylindrical modality;

# 3D full-scale modeling of an LPAs over cm to m scales is challenging task

laser wavelength ( $\lambda_0$ )	$\sim \mu\text{m}$
laser length (L)	$\sim$ few tens of $\mu\text{m}$
plasma wavelength ( $\lambda_p$ )	$\sim 10 \mu\text{m}$ @ $10^{19} \text{ cm}^{-3}$ $\sim 30 \mu\text{m}$ @ $10^{18} \text{ cm}^{-3}$ $\sim 100 \mu\text{m}$ @ $10^{17} \text{ cm}^{-3}$
interaction length (D)	$\sim \text{mm}$ @ $10^{19} \text{ cm}^{-3} \rightarrow 100 \text{ MeV}$ $\sim \text{cm}$ @ $10^{18} \text{ cm}^{-3} \rightarrow 1 \text{ GeV}$ $\sim \text{m}$ @ $10^{17} \text{ cm}^{-3} \rightarrow 10 \text{ GeV}$

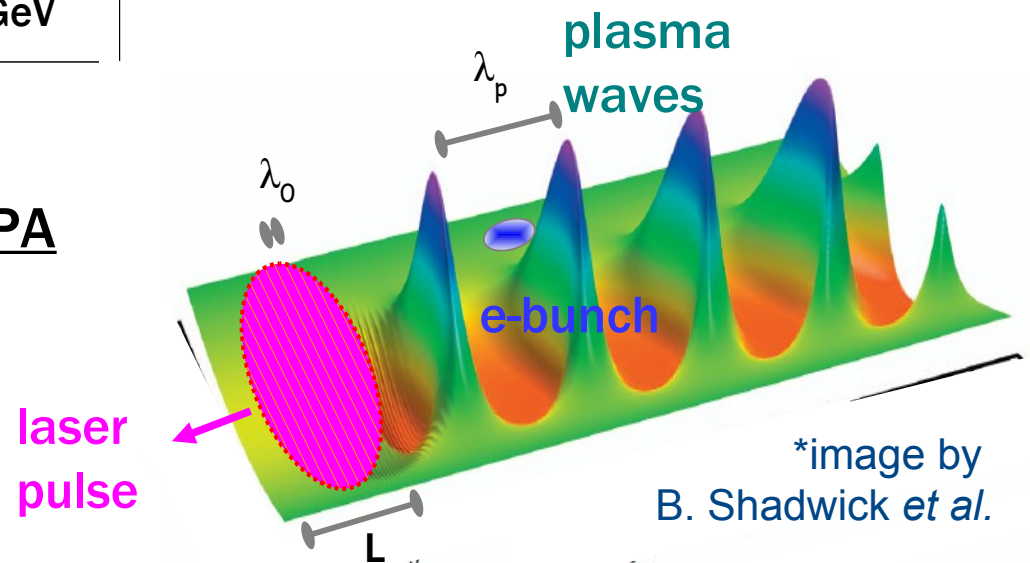
- Simulation complexity  $\sim (D/\lambda_0)^{4/3}$
- Cost of 3D explicit PIC simulations:
  - $10^4$ - $10^5$  CPUh for 100 MeV stage
  - $\sim 10^6$  CPUh for 1 GeV stage
  - $\sim 10^7$  - $10^8$  CPUh for 10 GeV stage

## Ex: Full 3D PIC modeling of 10 GeV LPA

grid:  $5000 \times 500^2 \sim 10^9$  points

particles:  $\sim 4 \times 10^9$  particles (4 ppc)

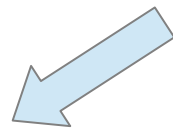
time steps:  $\sim 10^7$  iterations



# Understanding the physics of LPAs requires detailed numerical modeling

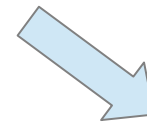
What we need (from the computational point of view):

- run 3D simulations (dimensionality matters!) of cm/m-scale laser-plasma interaction in a reasonable time (a few hours/days)
- perform, for a given problem, **several simulations** (exploration of the parameter space, optimization, convergence check, comparison with experiments, feedback with experiments for optimization, etc.)



## Reduced Models

→ Neglecting some aspects of the physics depending on the particular problem that needs to be addressed, (reducing computational complexity)



## Lorentz Boosted Frame

→ Different spatial/temporal scales in an LPA simulation do not scale the same way changing the reference frame. Simulation length can be greatly reduced going to an optimal (wake) reference frame.

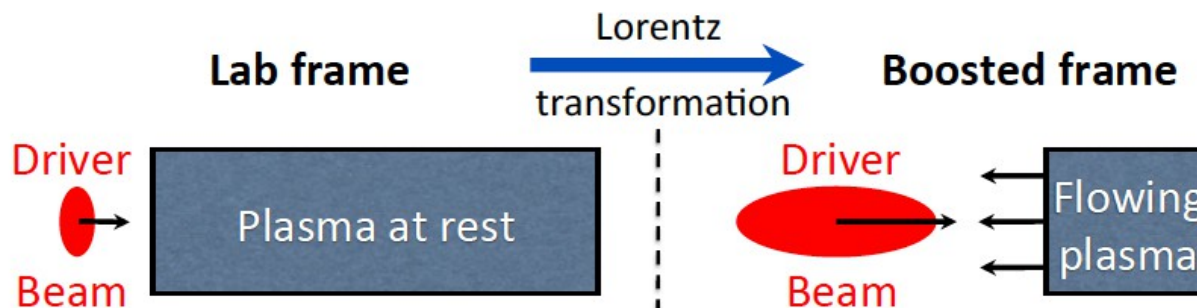
# Modeling in a Lorentz boosted frame

# Modeling an LPA in a Lorentz boosted frame

The space/time scales spanned by a system are not invariant under Lorentz transform  
 → the computational complexity of the problem can be reduced changing the reference frame

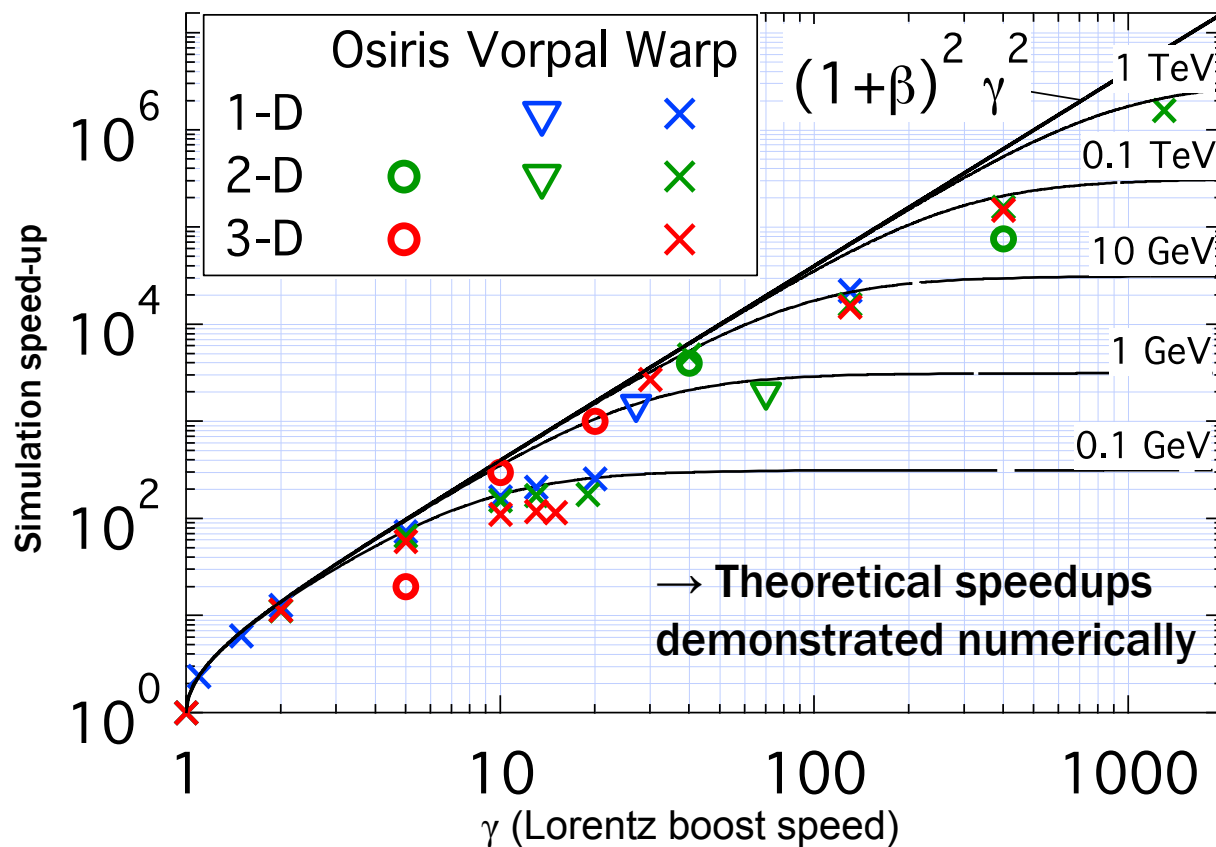
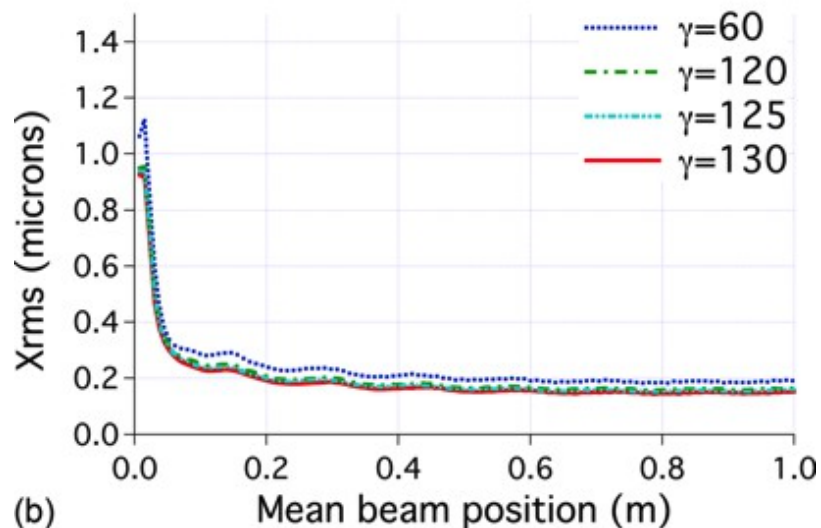
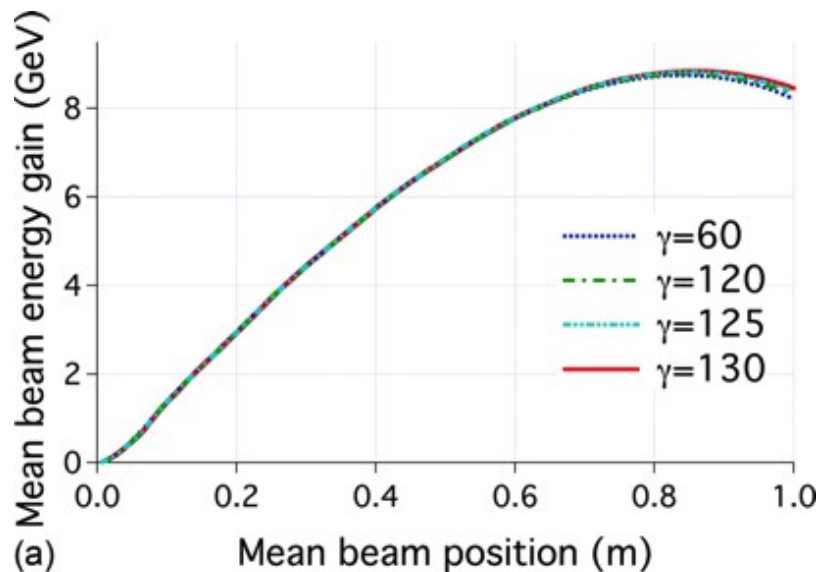
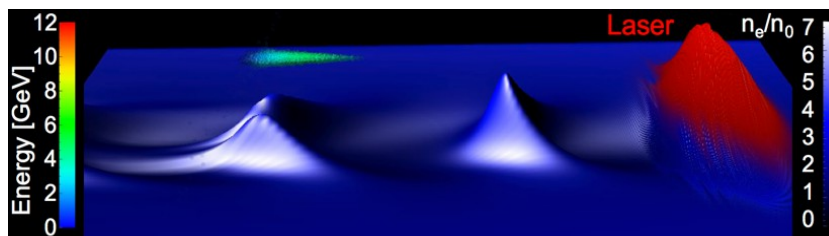
Laboratory Frame	Boosted Lorentz Frame ( $\beta_*$ )
$\lambda_0 \rightarrow$ laser wavelength $\ell \rightarrow$ laser length $L_p \rightarrow$ plasma length $c\Delta t < \Delta z \ll \lambda_0, \lambda_0 < \ell \ll L_p$	$\lambda'_0 = \gamma_*(1 + \beta_*) \lambda_0 > \lambda_0$ $\ell' = \gamma_*(1 + \beta_*) \ell > \ell$ $L'_p = L_p/\gamma_* < L_p$
$\Rightarrow t_{simul} \sim (L_p + \ell)/c$ $\# \text{ steps} = \frac{t_{simul}}{\Delta t} \propto \frac{L_p}{\lambda_0} \gg 1$ <b>large # of steps</b>	$\Rightarrow t'_{simul} \sim (L'_p + \ell')/(c(1 + \beta_*))$ $\# \text{ steps}' = \frac{t'_{simul}}{\Delta t'} \propto \frac{L_p}{\lambda_0 \gamma_*^2 (1 + \beta_*)^2}$ <b># of steps reduced (<math>1/\gamma_*^2</math>)</b>

- Neglects backward propagating waves (blueshifted and so under-resolved in the BF);
- Diagnostic and initialization are more complicated;
- For any LPA there is an “optimal” frame, the frame of the wake:  $\gamma_{opt} \sim k_0/k_p$   
 $\rightarrow S \sim (\lambda_p/\lambda_0)^2$



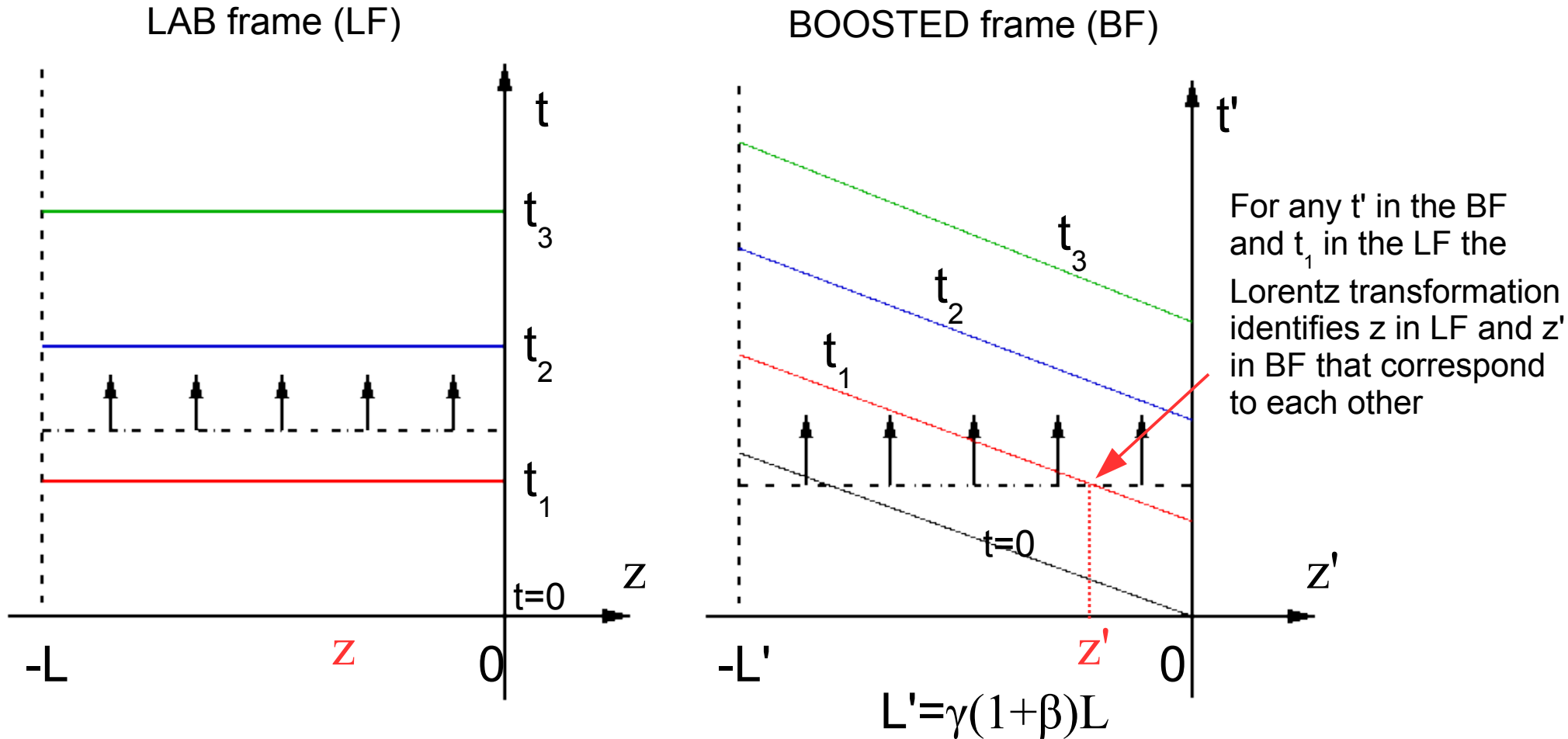
# Modeling an LPA in the BF provides large computational gains

Modeling of a ~10 GeV LPA stage



Simulation cost for 10 GeV LPA (3D) w/ WARP:  
5,000 CPUh using LBF (reduction ~20,000)

# Simulation initialization and diagnostics in the Lorentz boosted Frame

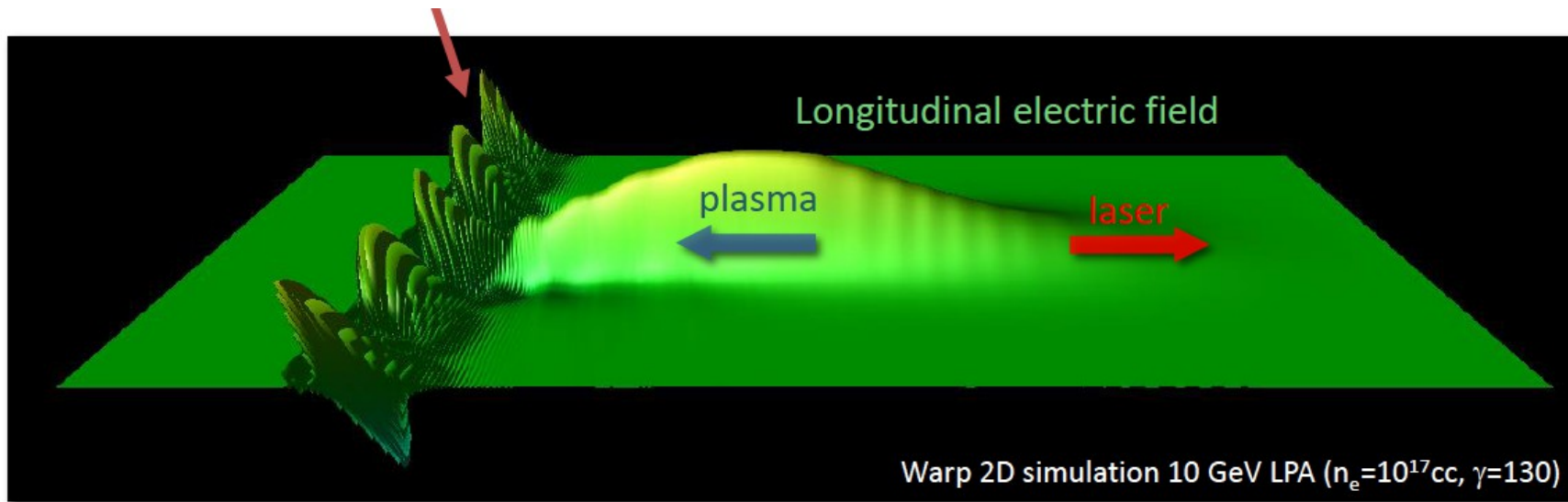


Initializing the simulation in the BF and obtaining output (diagnostics) in the LF while performing the simulation in the BF is challenging due to the mixing between space and time among BF and LF → **use a moving planar antenna**



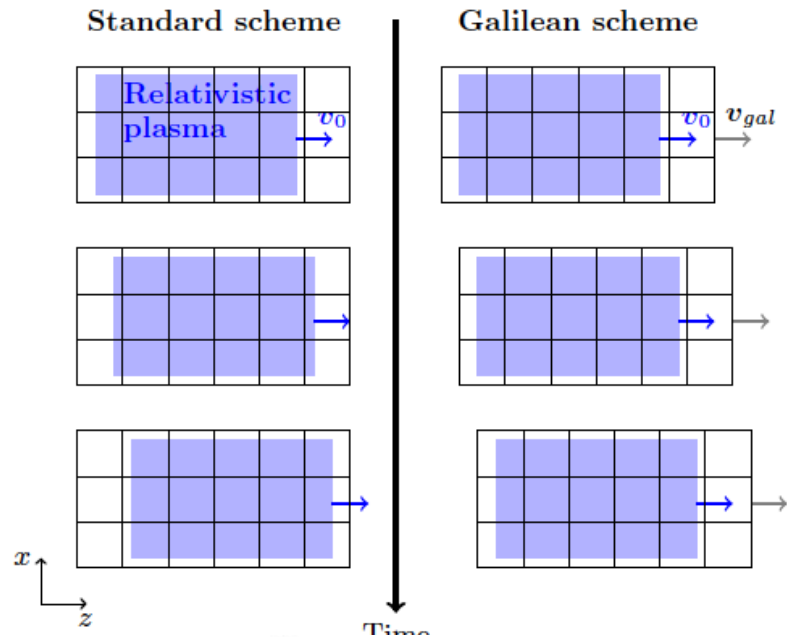
# Numerical Cherenkov Instability (NCI) prevents realization of the full potential of BF simulations

Snapshot of the electron density in a BF simulation

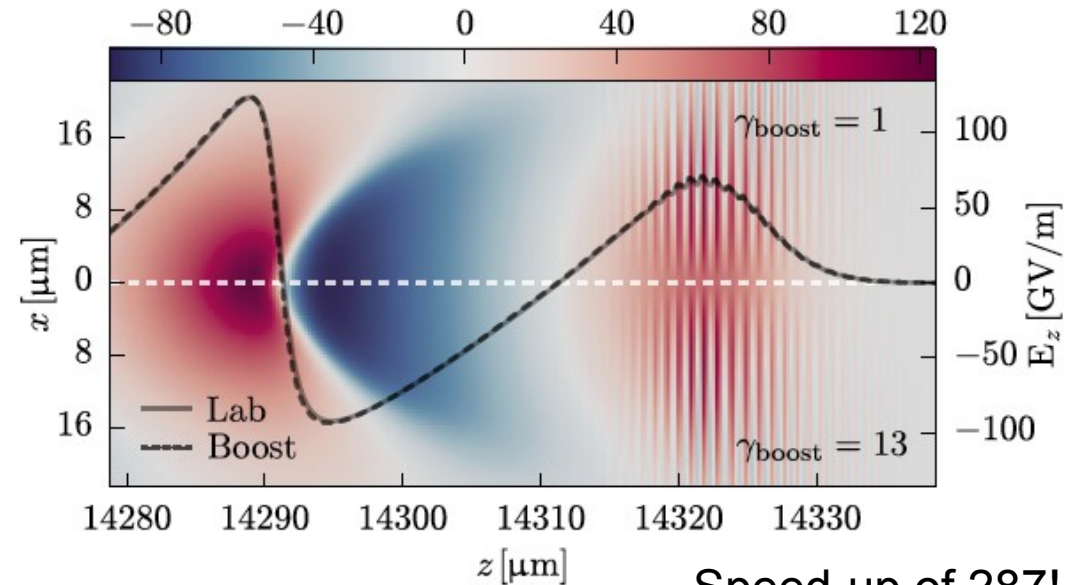
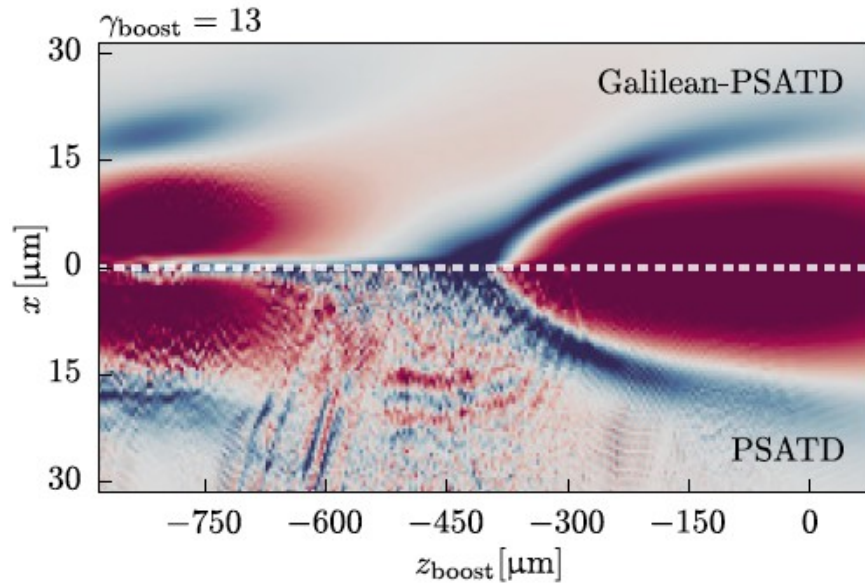


- NCI in PIC codes arises from coupling between distorted EM modes (e.g., EM with slow phase velocity) and spurious beam modes (drifting plasma);
- NCI prevents use of high boost velocities;
- Several solutions proposed over the years to mitigate the instability (see References) involving strong digital smoothing (filtering EM fields/currents) or arbitrary numerical corrections which are tuned specifically against the NCI and go beyond the natural discretization of the equations;
- Elegant solution found by M. Kirchen (DESY) and R. Lehe (LBNL) that completely eliminates NCI without an *ad hoc* assumption or treatment of the physics →

# NCI can be eliminated by rewriting PIC equations using a coordinates system (Galilean transform) co-moving with the drifting plasma



- PIC equations rewritten using a coordinates system co-moving with the plasma (Galilean transform):  $z' = z - v_0 t$  ( $v_0$  velocity of drifting plasma in BF)
  - Use PSATD scheme (i.e., solve Maxwell's equation in Fourier space + analytical integration over  $\Delta t$ )
- Intrinsically free of NCI for drifting plasma



Speed-up of 287!

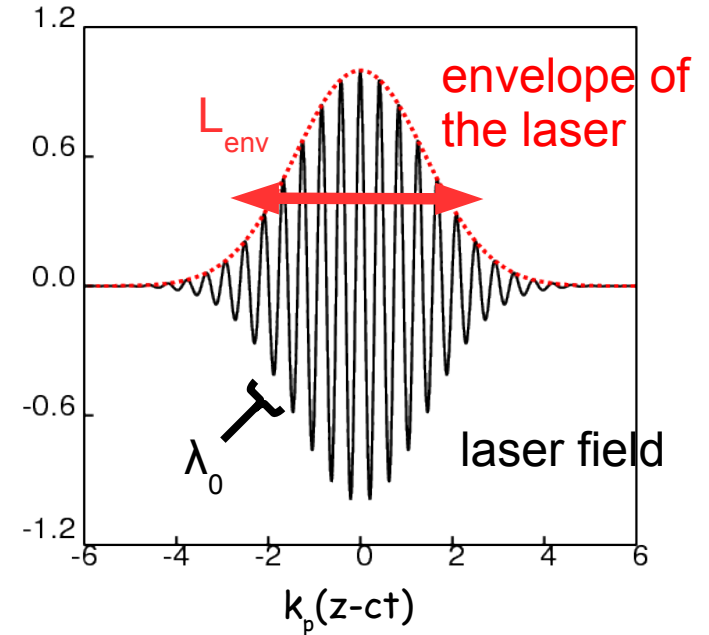
# Laser-envelope description

# Laser-envelope description (pond. guiding center)

- In an LPA, the laser envelope usually satisfies  $L_{\text{env}} (\sim 10\text{s of } \mu\text{m}) \gg \lambda_0 (\sim 1 \mu\text{m})$
- Plasma electrons quiver in the fast laser field
- There is a time scale separation between the fast laser fields ( $\omega_0$ ) and the slow wakefield ( $\omega_p$ ), typically  $\omega_p \ll \omega_0$

→ **ponderomotive approximation**: electron motion averaged (analytically) over fast laser oscillations

→ laser **decomposed** into fast phase and slow envelope, only the latter is evolved



Laser vector potential → 
$$a_{\perp}(\zeta, \tau) = \frac{\overbrace{\hat{a}(\zeta, \tau)}^{\text{slow}} \overbrace{e^{ik_0\zeta}}^{\text{fast}}}{2} + \text{c.c.}$$

Electron equation of motion → 
$$\frac{d\mathbf{p}}{dt} = \underbrace{-\frac{mc^2}{4\bar{\gamma}} \nabla |\hat{a}|^2}_{\text{averaged ponderomotive force}} - e \underbrace{\left( \mathbf{E} + \frac{\mathbf{v}}{c} \times \mathbf{B} \right)}_{\text{wake contribution}} \quad \bar{\gamma} = \left( 1 + \frac{|\mathbf{p}|^2}{m^2 c^2} + \frac{|\hat{a}|^2}{2} \right)^{1/2}$$

⇒ Envelope description removes scale @  $\lambda_0$  from the simulation [ $\sim (\lambda_p / \lambda_0)^2$  speed-up]  
 ⇒ Envelope generally axisymmetric → modeling in 2D cylindrical geometry possible

# Complete set of equations to be solved in an envelope code

Laser envelope equation

$$\left( \nabla_{\perp}^2 + 2i \frac{k_0}{c} \frac{\partial}{\partial \tau} + \frac{2}{c} \frac{\partial^2}{\partial \zeta \partial \tau} - \frac{1}{c^2} \frac{\partial^2}{\partial \tau^2} \right) \hat{a} = k_{p0}^2 \frac{\bar{n}}{n_0 \bar{\gamma}} \hat{a}$$

Laser driver and wake are decoupled (good for diagnostics)

Wakefield description (Maxwell equations) [slow fields  $\sim \omega_p$ ]

$$\frac{\partial \mathbf{E}}{\partial t} = c \nabla \times \mathbf{B} - 4\pi \mathbf{J} \quad \frac{\partial \mathbf{B}}{\partial t} = -c \nabla \times \mathbf{E}$$

Plasma description (equations of motion for numerical particles sampling the plasma)

$$\frac{d\mathbf{p}}{dt} = -\frac{mc^2}{4\bar{\gamma}} \nabla |\hat{a}|^2 - e \left( \mathbf{E} + \frac{\mathbf{v}}{c} \times \mathbf{B} \right) \quad \bar{\gamma} = \left( 1 + \frac{|\mathbf{p}|^2}{m^2 c^2} + \frac{|\hat{a}|^2}{2} \right)^{1/2}$$

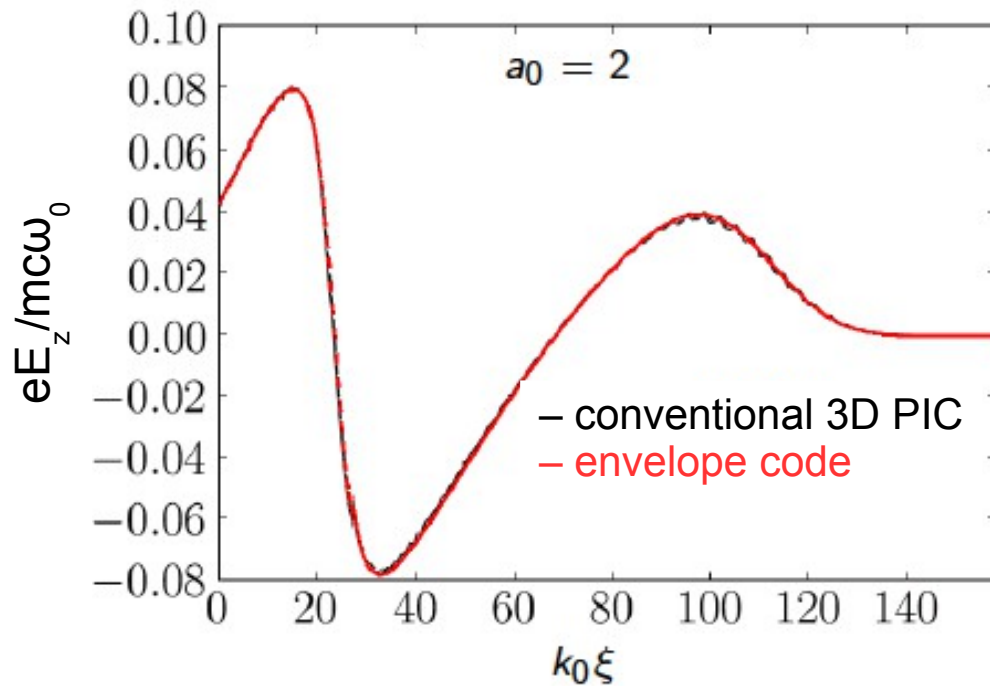
$$\frac{d\mathbf{r}}{dt} = \mathbf{v} = \frac{\mathbf{p}}{\bar{\gamma}}$$

→ coupling between the equations provided by  $\mathbf{J}$  and  $\bar{n}$

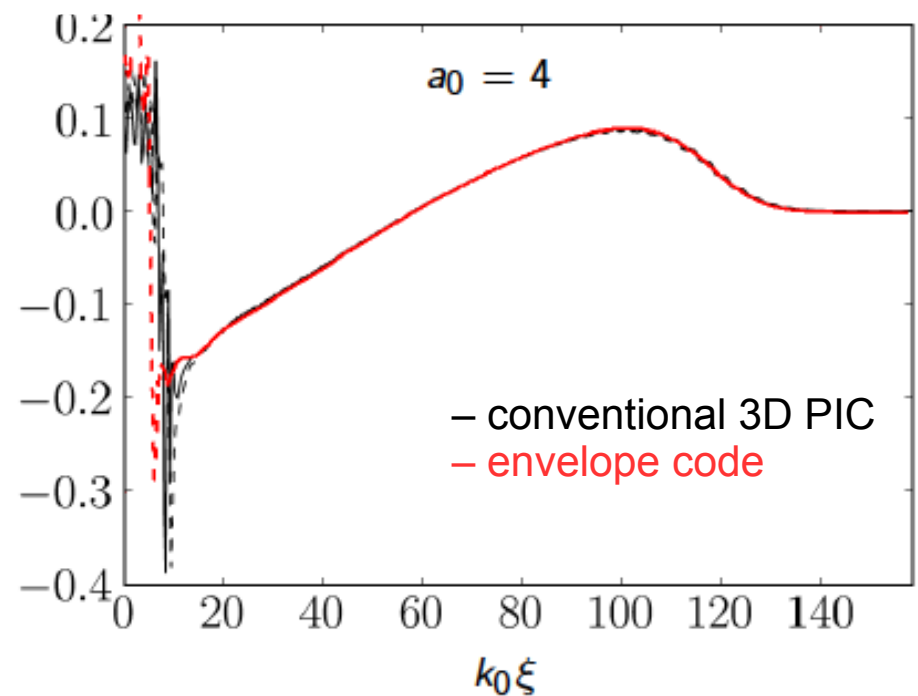
# Wakefield structure and amplitude in excellent agreement with results obtained with conventional 3D PIC

→ Lineout of the longitudinal wakefield,  $E_z$

### Quasi-linear wake



### Nonlinear wake



==> averaged ponderomotive approximation works **very well** for laser and plasma parameters of interest for current and future LPA experiments

# Envelope codes reproduce correct laser group velocity in vacuum and plasmas

Plasma profile:

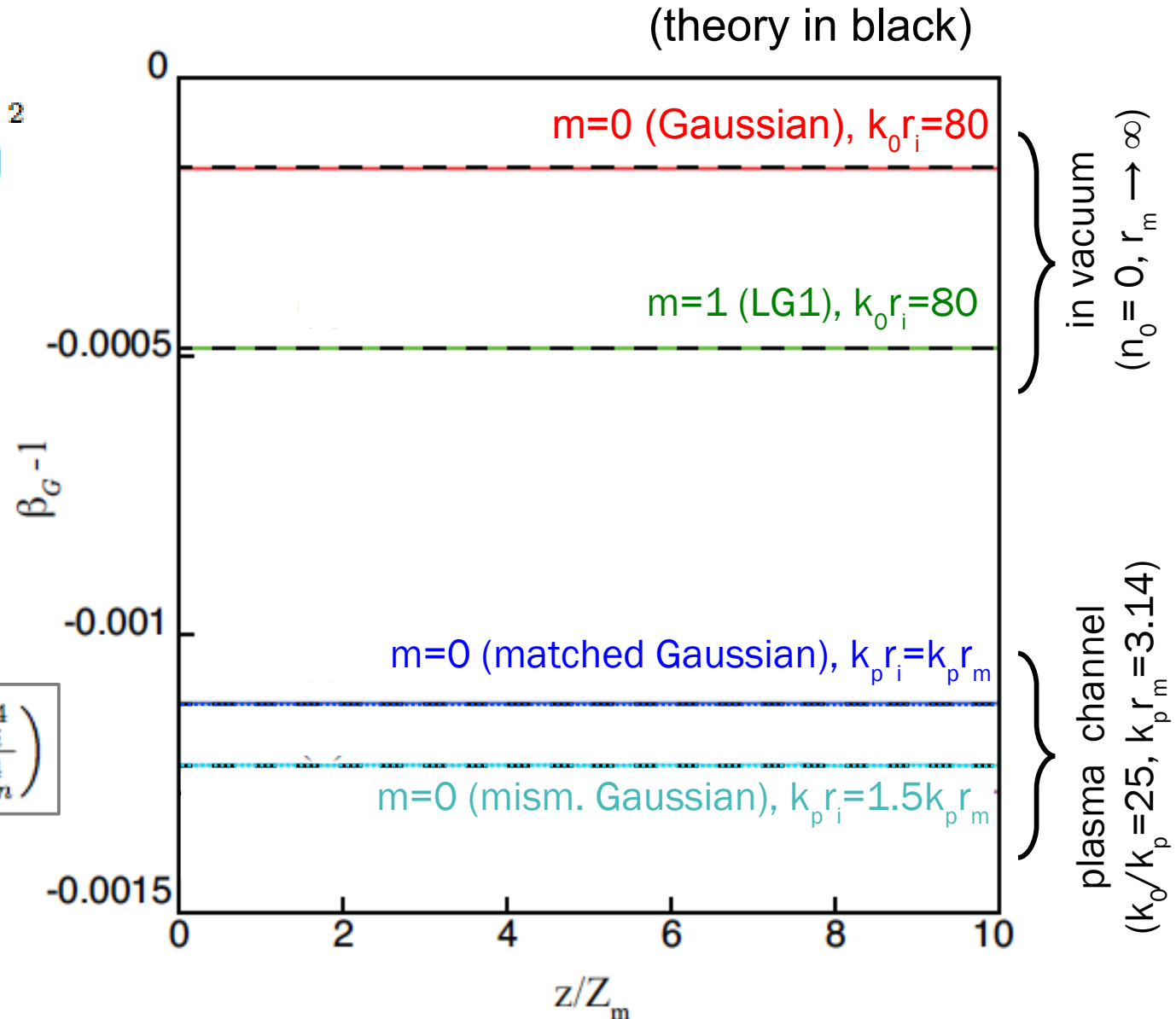
$$n(r) = n_0 + (\pi r_e r_m)^{-1} \left( \frac{r}{r_m} \right)^2$$

Laser profile:

$$\hat{a}_\perp \sim L_m^0 \left( \frac{2r^2}{w_0^2} \right) e^{-r^2/w_0^2}$$

Laser velocity:

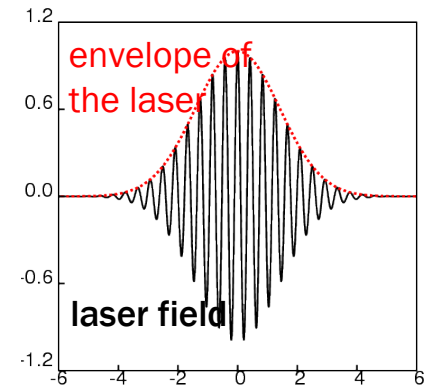
$$\beta_g = 1 - \frac{k_p^2}{2k_0^2} - \frac{1+2m}{k_0^2 r_i^2} \left( 1 + \frac{r_i^4}{r_m^4} \right)$$



# Correct numerical modeling of a strongly depleted laser pulse is challenging

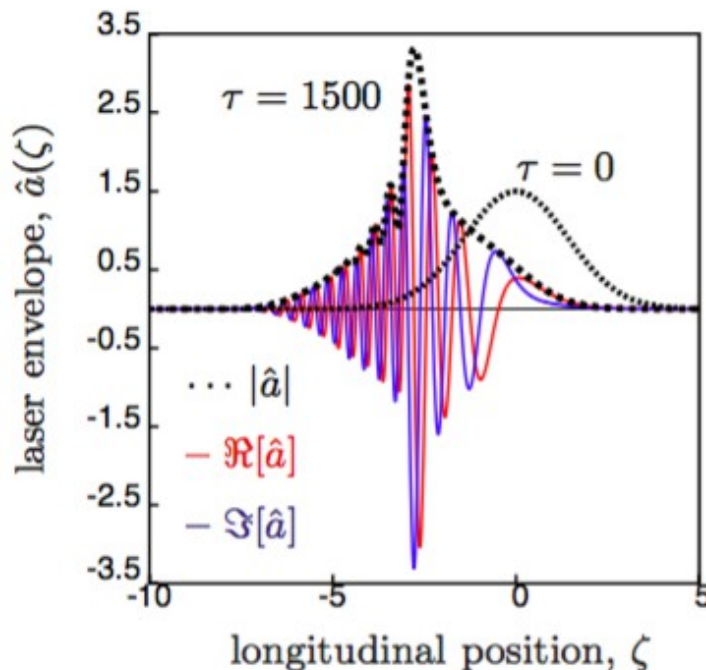
Envelope description:  $a_{\text{laser}} = \hat{a} \exp[ik_0(z-ct)]/2 + \text{c.c.}$

$$\left( \nabla_{\perp}^2 + 2i \frac{k_0}{c} \frac{\partial}{\partial \tau} + \frac{2}{c} \frac{\partial^2}{\partial \zeta \partial \tau} - \frac{1}{c^2} \frac{\partial^2}{\partial \tau^2} \right) \hat{a} = k_{p0}^2 \frac{\bar{n}}{n_0 \bar{\gamma}} \hat{a}$$



- early times: NO need to resolve  $\lambda_0$  ( $\sim 1 \mu\text{m}$ ), only  $L_{\text{env}} \sim \lambda_p$  ( $\sim 10\text{-}100 \mu\text{m}$ )
- later times: spectral modification (i.e., laser-pulse redshifting)  $\rightarrow$  structures **smaller** than  $L_{\text{env}}$  **arise** in  $\hat{a}$  (mainly in  $\text{Re}[\hat{a}]$  and  $\text{Im}[\hat{a}]$ ) and **need to be captured\***

$a_0 = 1.5$   
 $k_0/k_p = 20$   
 $L_{\text{env}} = 1$



Is it possible to have a good description of a depleted laser at a “reasonably low” resolution (in space and time)?

\*Benedetti *et al.*, AAC2010  
 Cowan *et al.*, JCP (2011)  
 Zhu *et al.*, POP (2012)



# Ingredients for an efficient laser envelope solver

- Envelope evolution equation discretized in time using a 2<sup>nd</sup> order Crank-Nicholson implicit scheme → **enable large time steps**

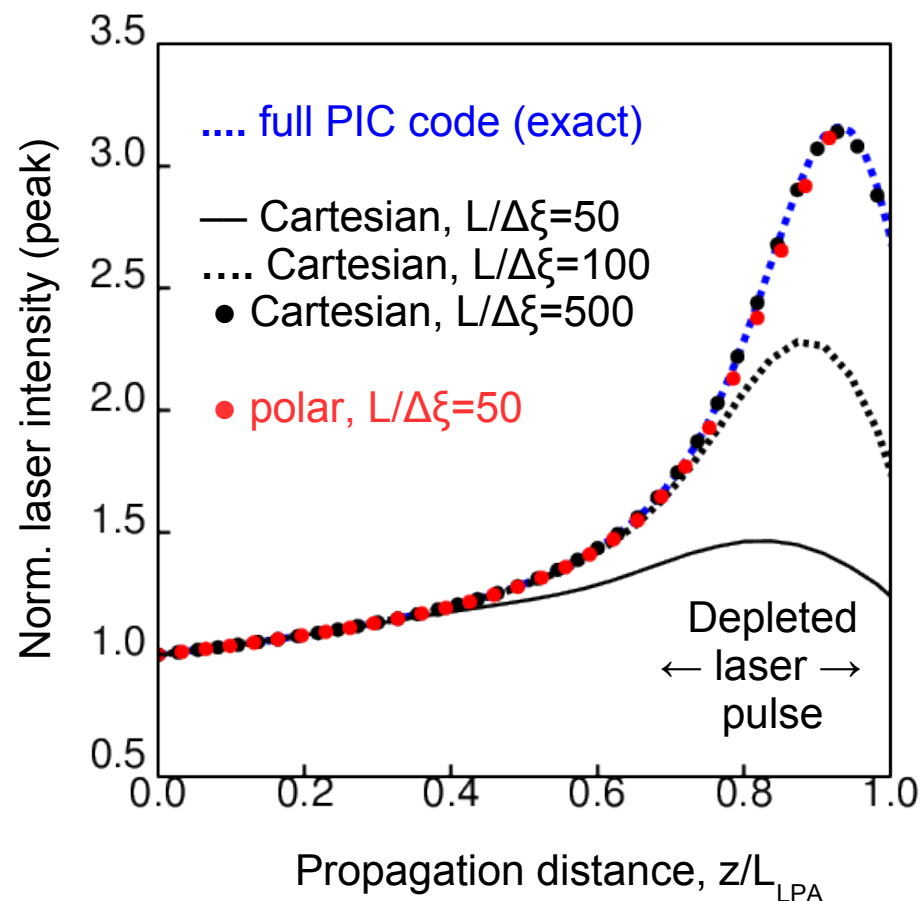
$$-\frac{\hat{a}^{n+1} - 2\hat{a}^n + \hat{a}^{n-1}}{\Delta\tau^2} + 2 \left( i \frac{k_0}{k_p} + \frac{\partial}{\partial \xi} \right) \frac{\hat{a}^{n+1} - \hat{a}^{n-1}}{2\Delta\tau} = -\nabla_{\perp}^2 \frac{\hat{a}^{n+1} + \hat{a}^{n-1}}{2} + \frac{\delta^n}{\gamma_{\text{fluid}}^n(\hat{a}^n)} \frac{\hat{a}^{n+1} + \hat{a}^{n-1}}{2}$$

- Use a **polar** representation for  $\hat{a}$  when computing  $\partial/\partial\xi$

$$\hat{a} = \overset{\text{(cartesian)}}{\Re[\hat{a}]} + i \overset{\text{(cartesian)}}{\Im[\hat{a}]} = \overset{\text{(polar)}}{|\hat{a}|} e^{i\theta}$$

$$\partial_{\xi} \hat{a} = \begin{cases} \overset{\text{(cartesian)}}{\partial_{\xi} (\Re[\hat{a}]) + i \partial_{\xi} (\Im[\hat{a}])} \\ \overset{\text{(polar)}}{\underbrace{\partial_{\xi} (|\hat{a}|)} e^{i\theta} + i (\partial_{\xi} \theta) \hat{a}} \end{cases}$$

“smoother” behavior compared to  $\text{Re}[\hat{a}]$  and  $\text{Im}[\hat{a}]$  → **easier to differentiate numerically!**



# Modeling performed with 2D-cylindrical envelope scheme provides significant speedup compared to full 3D PIC still retaining physical fidelity

$n_0$ [e/cm <sup>3</sup> ]	$k_0/k_p$	$a_0$	$\tau$ [fs]	$w_0$ [ $\mu$ m]	$L_{sym}$ [mm]
$3 \cdot 10^{18}$	24	5	30	16	3.2

box:  $23 \times 20$  - res:  $1/30 \times 1/20$  -  $\Delta t = 0.25\Delta z$  -

**Envelope code > 300 times faster than 3D explicit PIC code**

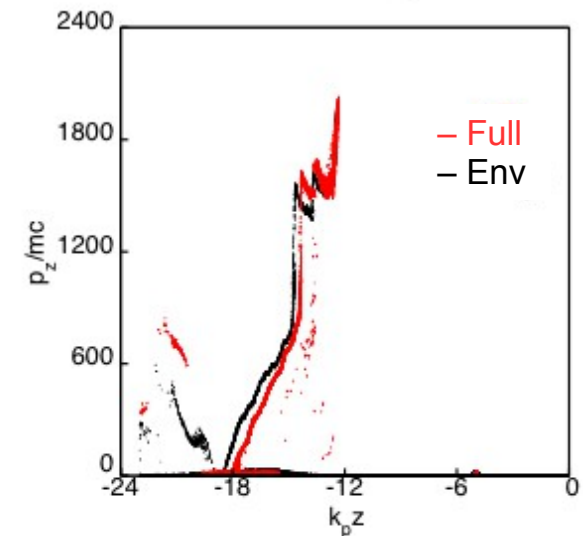
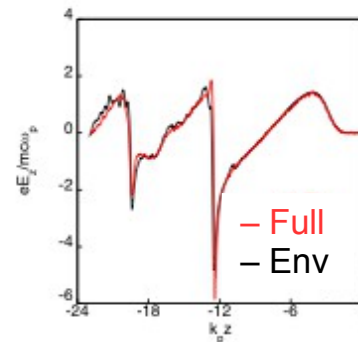
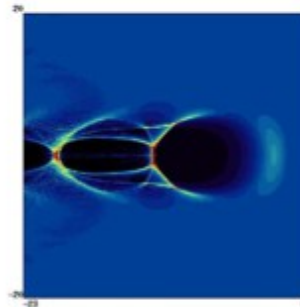
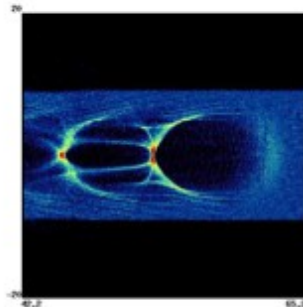
Full

Envelope

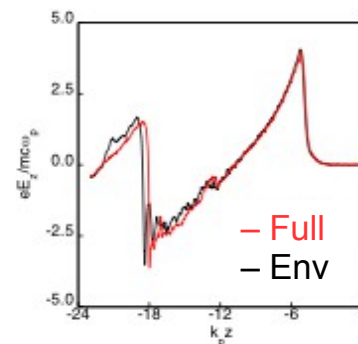
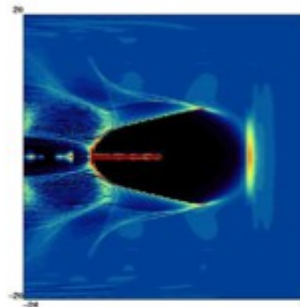
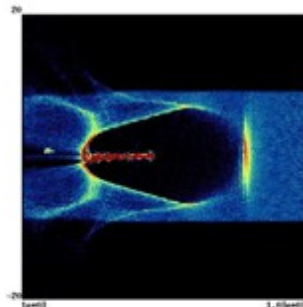
longitudinal field

long. phase space ( $ct = 3$  mm)

$ct = 0$  mm

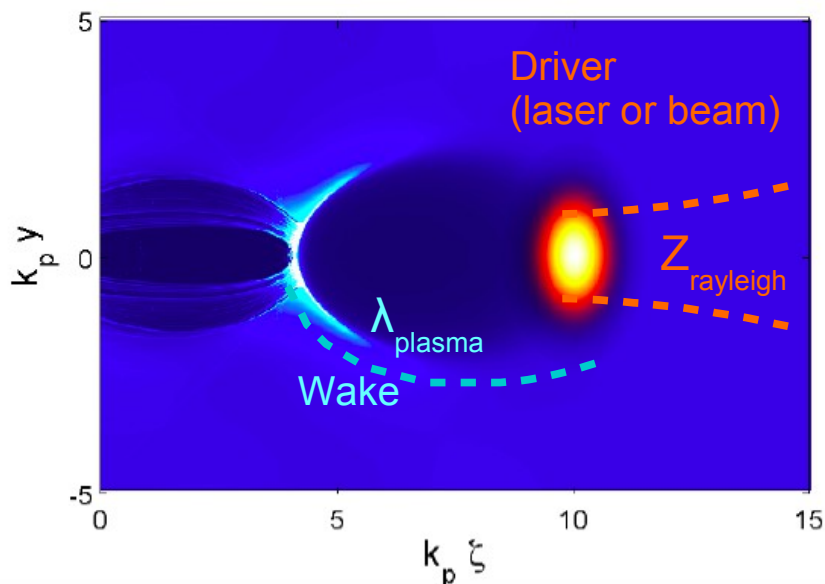


$ct = 3$  mm



# Quasi-static approximation

# Quasi-static approximation takes advantage of the time scale separation between driver and plasma evolution



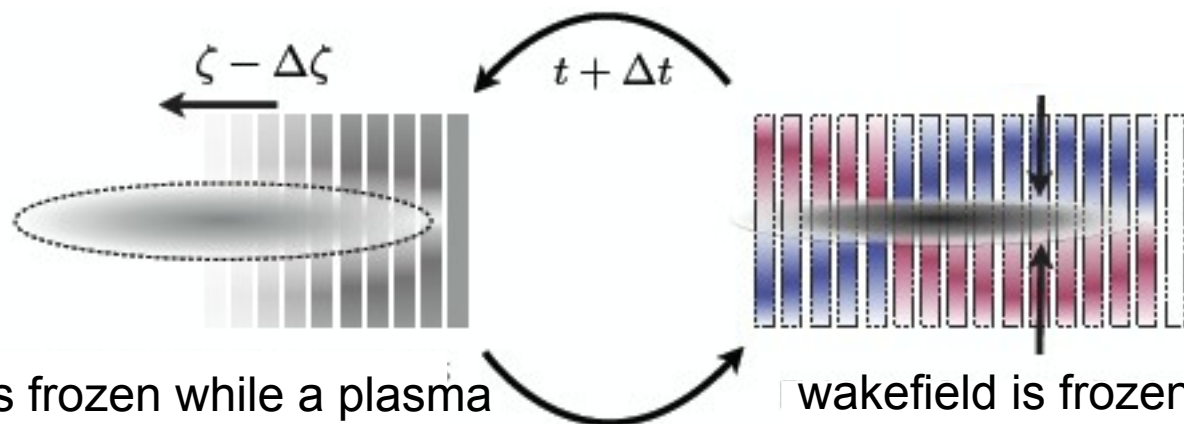
The laser (or beam) driver is evolving on a time scale much longer compare to the plasma response

$$T_{laser} \sim Z_{rayleigh}/c$$

$$T_{plasma} \sim \omega_p^{-1}$$

$$T_{laser}/T_{plasma} \sim (k_0/k_p)(k_p w_0)^2 \gg 1$$

- **neglect** time-dependence in all the quantities related to the **wake**
- **retain** time-dependence only in the evolution of the **driver**



Driver is frozen while a plasma slice is passed through the driver and the wakefield is computed

wakefield is frozen while driver is advanced in time

$\Delta t$  set according to driver evolution (much bigger than in conv. PIC):  
# of time steps reduced by  $\sim (\lambda_p/\lambda_0)^2$

\*Sprangle, et al., PRL (1990)  
Mora, Antonsen, Phys. Plas. (1997)

# Outline of the wake calculation in the quasi-static approximation (different in different codes)

1. Determine position and momentum of plasma particles on slice  $\zeta$  (computed from  $\zeta+d\zeta$ )

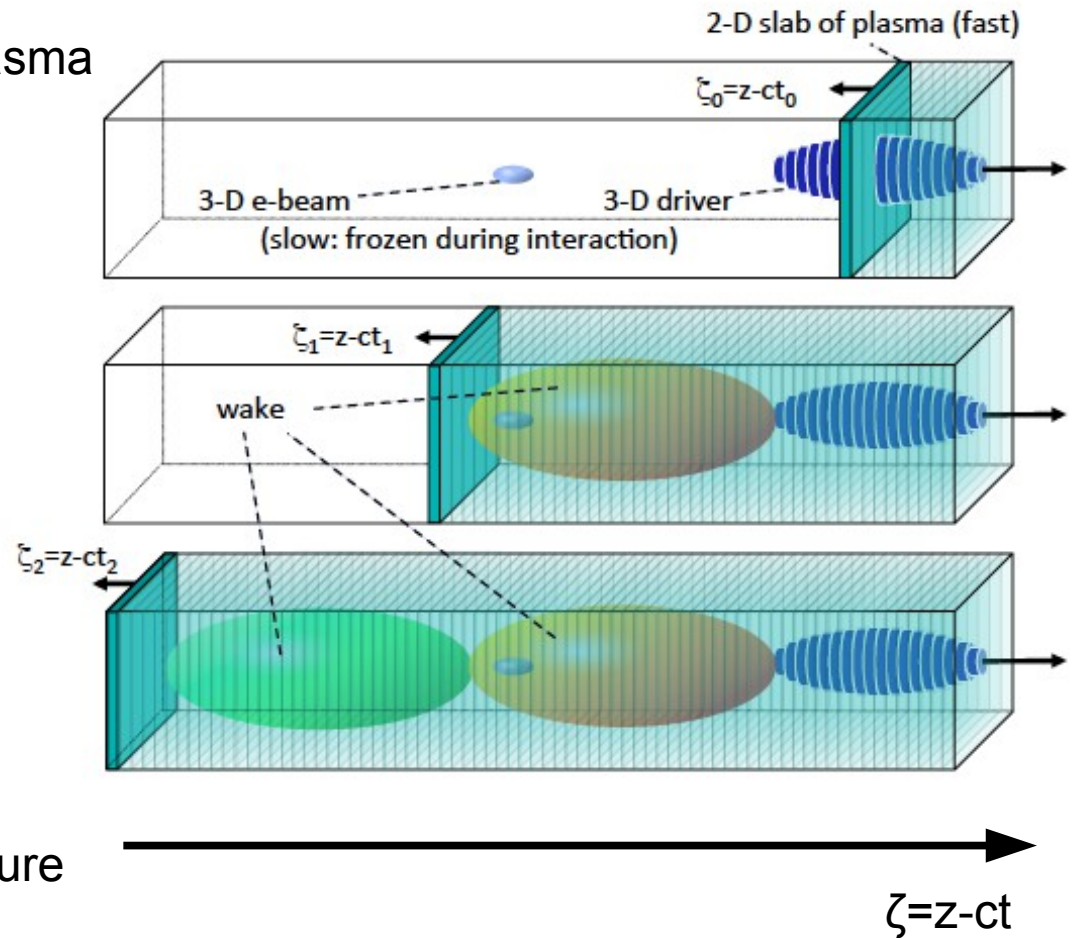
$$\begin{cases} \frac{dr}{d\xi} = -\frac{u_r}{1+\psi} \\ \frac{du_r}{d\xi} = \frac{F_{laser} + \gamma(E_r - B_\phi)}{1+\psi} + B_\phi \\ \frac{d\psi}{d\xi} = \frac{u_r}{1+\psi}(E_r - B_\phi) - E_z \\ \gamma - u_z - \psi = 1 \end{cases}$$

2. Deposit charge/current in the slice  $\zeta$

3. Solve PDEs for the fields in the slice  $\zeta$  (requires implementation of iterative procedure to obtain a solution)

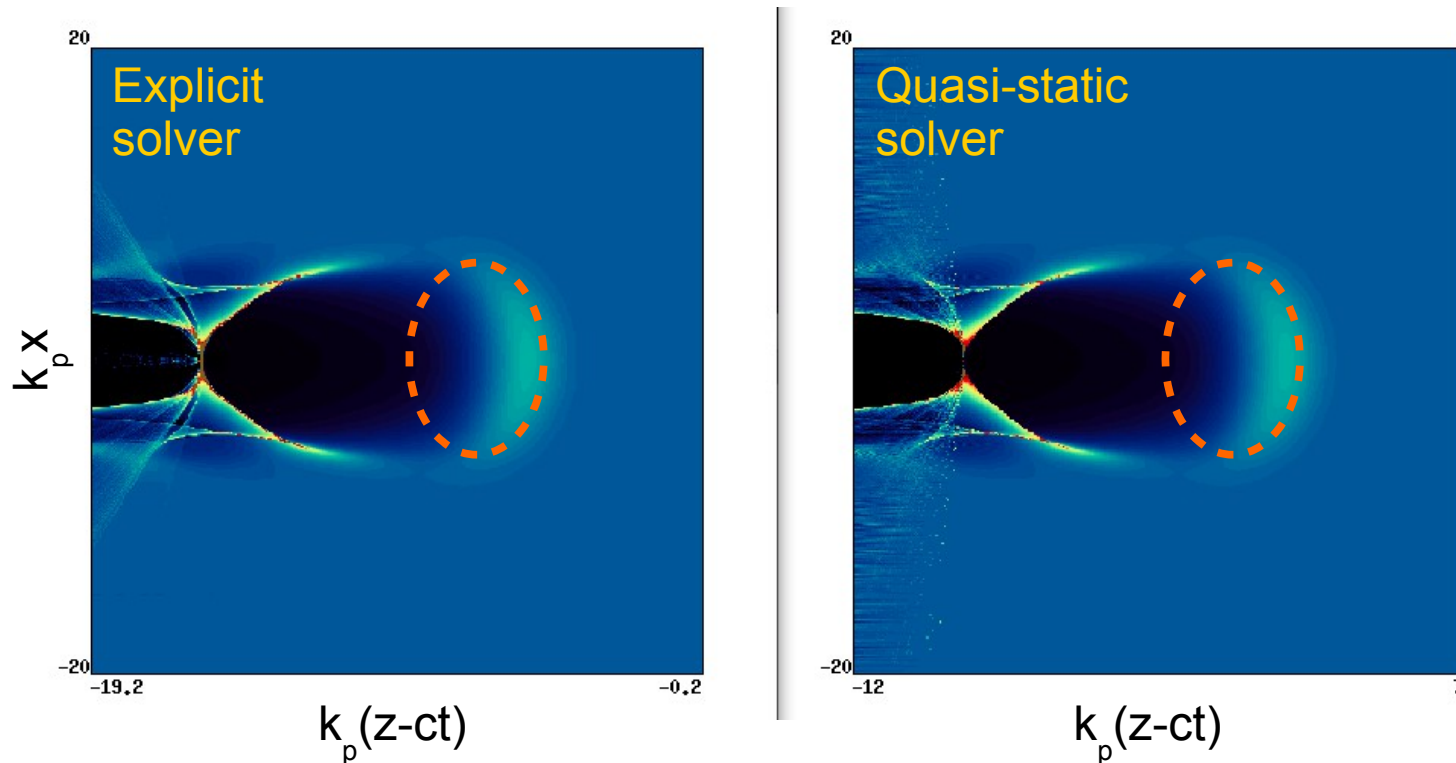
$$\nabla_{\perp}^2 E_z = \frac{1}{r} \frac{d}{dr} (rJ_r) \quad \frac{\partial(E_r - B_\phi)}{\partial \xi} = J_r \quad \frac{1}{r} \frac{d}{dr} (rB_\phi) = J_z - \frac{\partial E_z}{\partial \xi} \quad (\text{Poisson-like equations})$$

4. shift plasma slice (go to 1) and repeat until the end of the computational box is reached.



# Quasi-static approximation provides accurate description of the wakefield structure

Ex: bubble wake generated by an intense laser driver,  $a_0=5$



→ QSA particularly useful in describing dark-current-free LPA stages (bunch has to be provided): fast laser evolution and correct wake description

*N.B.* QSA solver **cannot** model some aspects of kinetic physics like particle self-injection (for trapped particles, plasma → bunch, the time scale separation does not hold)

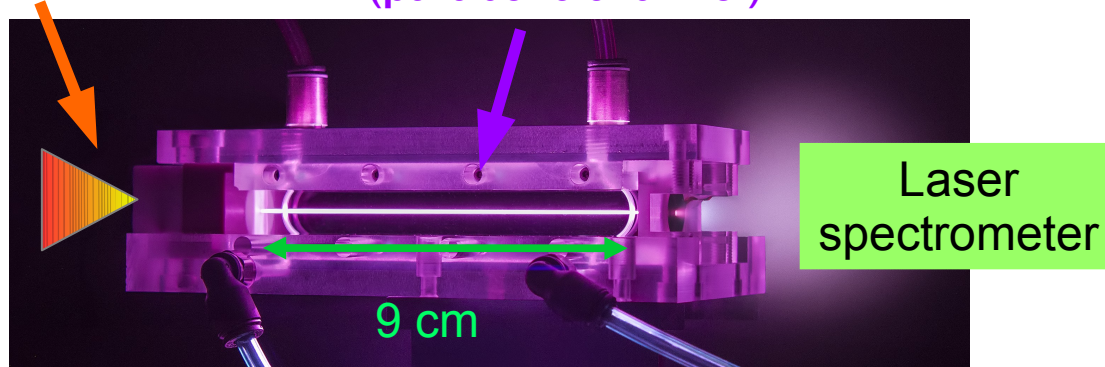
Laser envelope description (LED) +  
Quasi-static approximation (QSA):  
examples of the computational gains

# LED + QSA allow for detailed modeling of LPAs and close comparison with experiments/1

Comparison between measured and simulated post-interaction laser optical spectra used as independent density diagnostic\*.

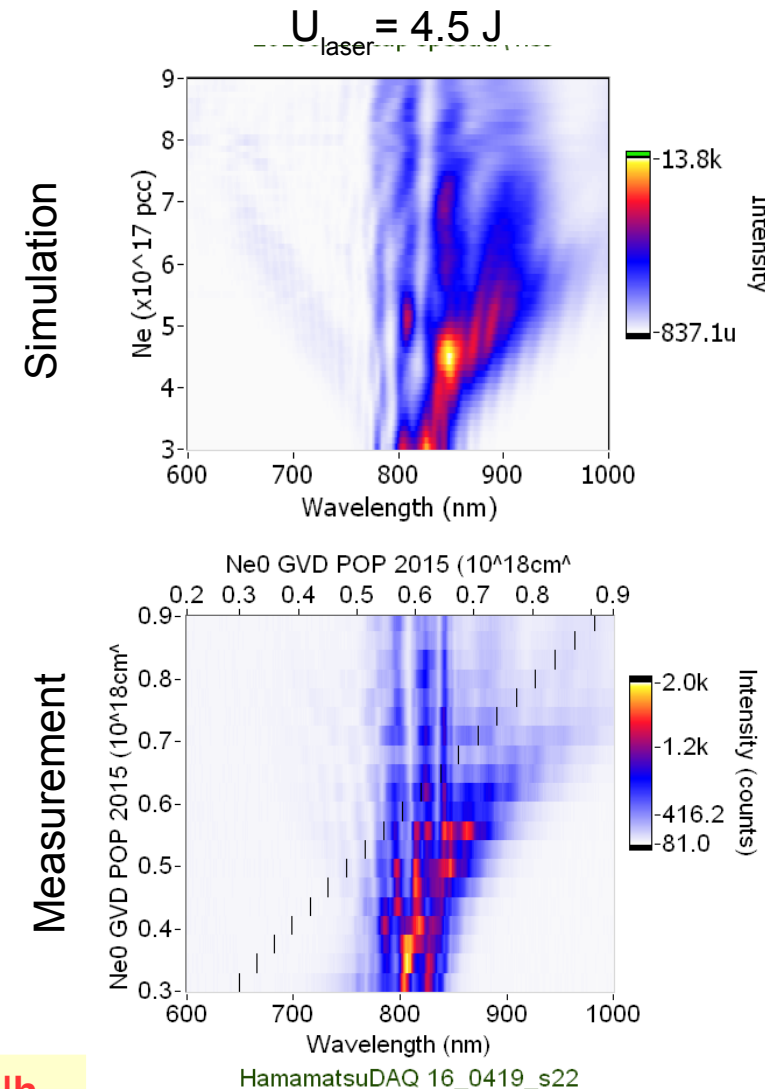
**Laser:**  
 $U = 4.5 \text{ J}$   
 $T = 30 \text{ fs}$   
 $w_0 = 53 \text{ } \mu\text{m}$

**Plasma (capillary):**  
 $L = 9 \text{ cm}$   
 $n_0 = (3-9) \times 10^{17} \text{ cm}^{-3}$   
(parabolic channel)



- 80 simulations (density scan) of a 9 cm LPA;
- modeling reproduces key features in laser spectra

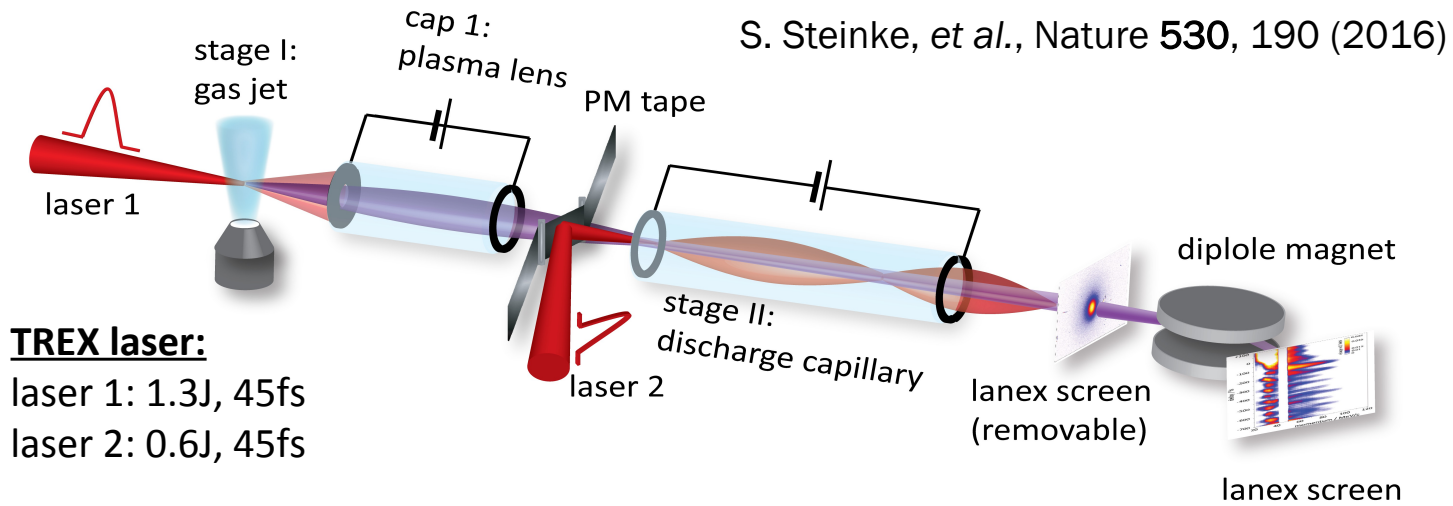
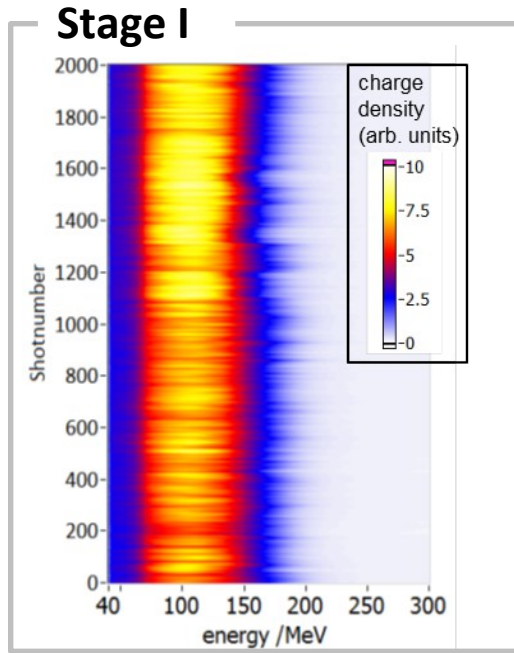
**9 cm LPA (nonlinear regime) simulation cost: ~10 CPUh**  
(reduction  $\sim 10^6$  compared to conventional 3D PIC)



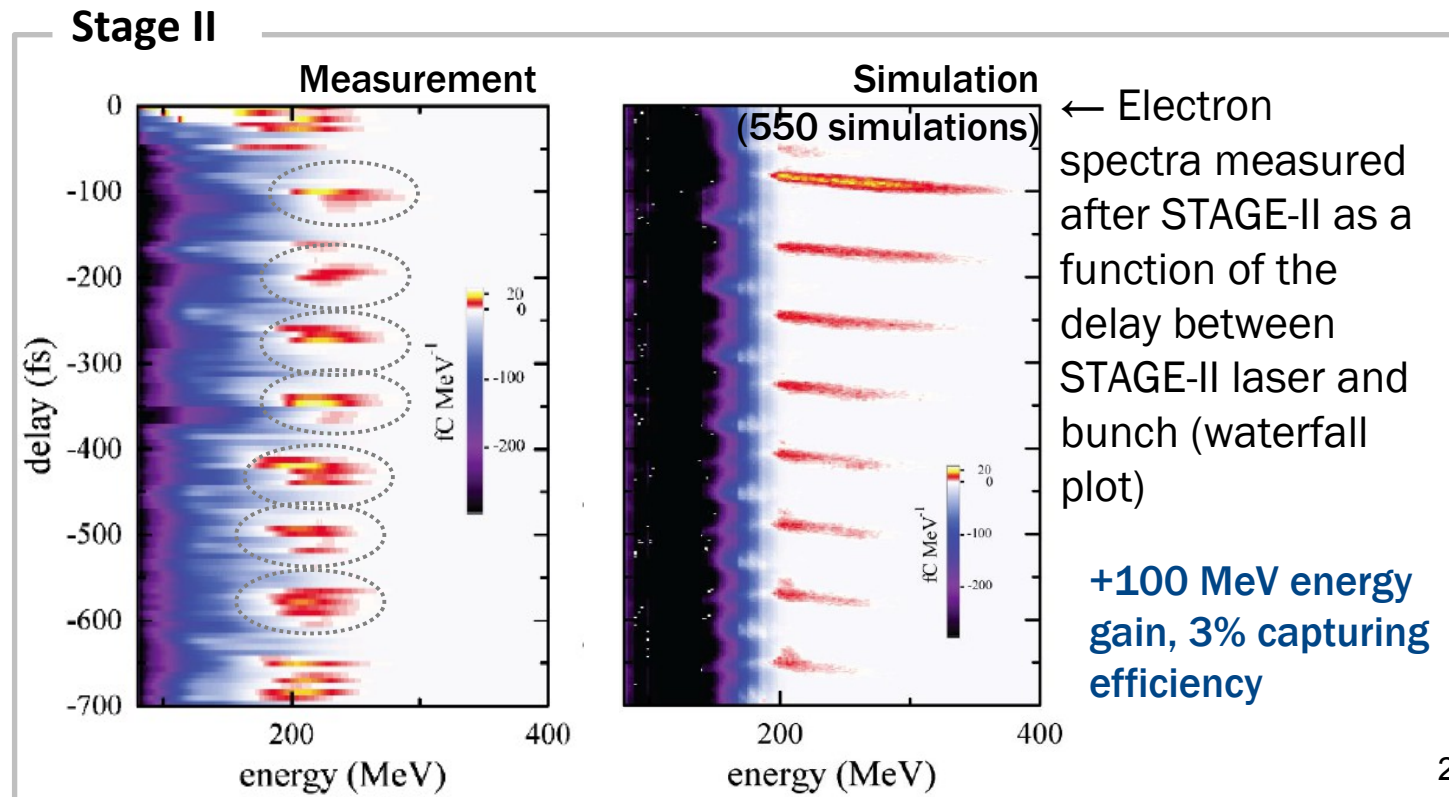


# LED + QSA allow for detailed modeling of LPAs and close comparison with experiments/2

Staging of independent LPAs.



**TREX laser:**  
 laser 1: 1.3J, 45fs  
 laser 2: 0.6J, 45fs

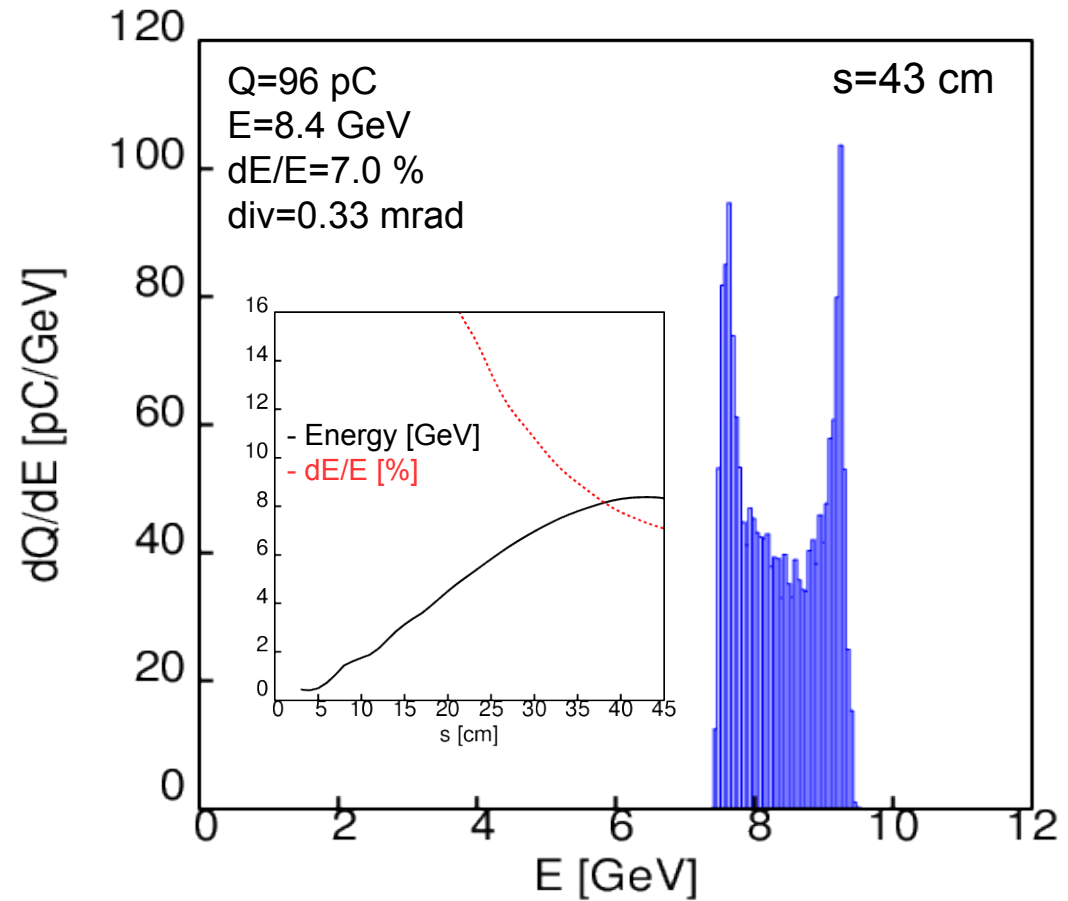
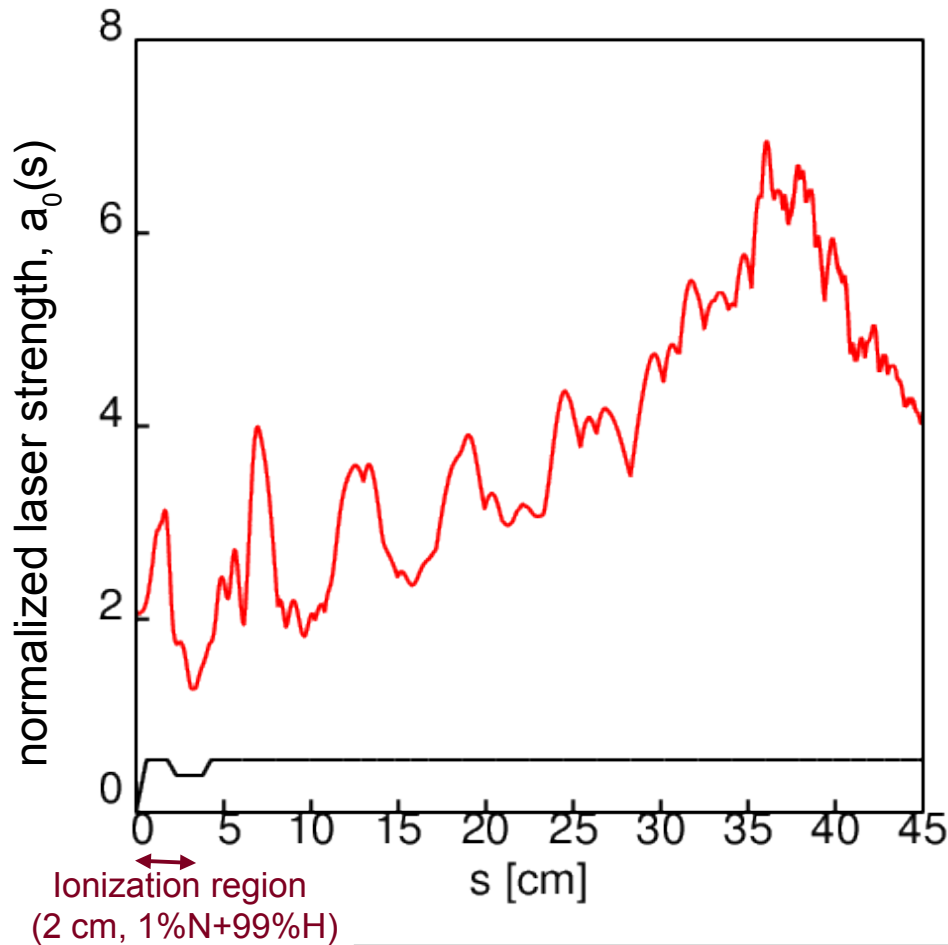


**Staging simulation cost:**  
 ~15 CPUh (reduction  
 ~60,000 compared to  
 conventional 3D PIC)

# LED + QSA allow for (very) efficient modeling of 10 GeV-class LPA stages in the quasi-linear regime

Laser (BELLA):  $U=36$  J,  $w_0=60$   $\mu\text{m}$  (spot size expanded w/ near field clipping),  $T=66$  fs

Plasma target: capillary discharge+laser heater (MHD)  $\rightarrow n_0=1.6 \times 10^{17}$   $\text{cm}^{-3}$ ,  $R_{\text{matched}}=70$   $\mu\text{m}$



**10 GeV simulation cost: ~50 CPUh (reduction  
~ $10^6$  compared to conventional 3D PIC code)**

N.B. No optimization for the injector (work in progress)

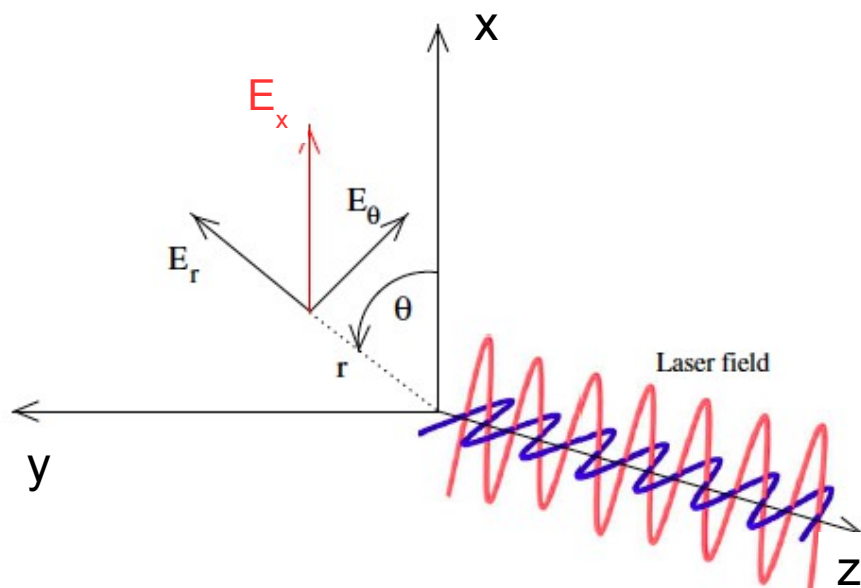
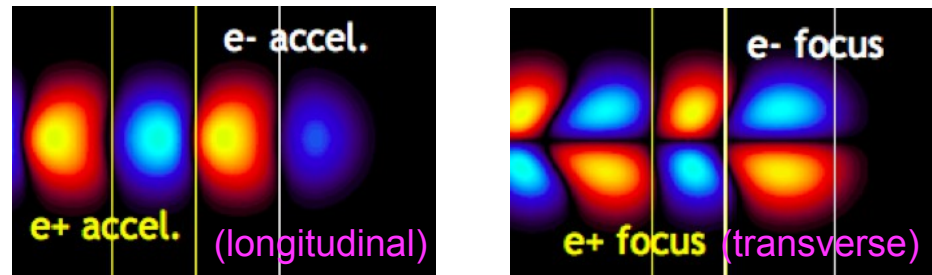
Quasi-cylindrical modality

# Motivation for a quasi-cylindrical modality

- Modeling of LPAs require a 3D description of the physics [laser evolution, wakefield structure, (self-)injection dynamics, etc.];
- For a driver with a **symmetric envelope**, the wake and laser field structure is “quasi-cylindrical”, i.e., when described in cylindrical geometry  $(z, r, \theta)$  it contains a **few** azimuthal modes (simple functional dependence from  $\theta$ )

Wake  $\rightarrow$  (almost) symmetric

Laser polarized along x  $\rightarrow$



Symmetric pulse  $[r=(x^2+y^2)^{1/2}]$

$$\begin{aligned}
 \mathbf{E} &= E_0(r, \zeta) \hat{x} \\
 &= \underbrace{\cos \theta E_0(r, \zeta)}_{E_r} \hat{r} - \underbrace{\sin \theta E_0(r, \zeta)}_{E_\theta} \hat{n}
 \end{aligned}$$

Simple  $\theta$ -dependence

# The Quasi-cylindrical (quasi-3D) modality: overview

- Represent the fields in cylindrical coordinates using a Fourier decomposition in  $\theta$

$$E_r(z, r, \theta) = \hat{E}_{r,0}(z, r) + \hat{E}_{r,1}(z, r)e^{i\theta} + \hat{E}_{r,2}(z, r)e^{2i\theta} + \dots$$

- similar expressions for all the components of  $\mathbf{E}$ ,  $\mathbf{B}$  and  $\mathbf{J}$
- truncate the series at a **low** order (usually 1 or 2) [**quasi-cylindrical assumption!**]
- use 2D (z,r) grids to represent the “coefficients”  $\hat{E}_{r,m}(z,r)$  for all the fields [gridless in  $\theta$ ]

- Solve Maxwell's equations\*

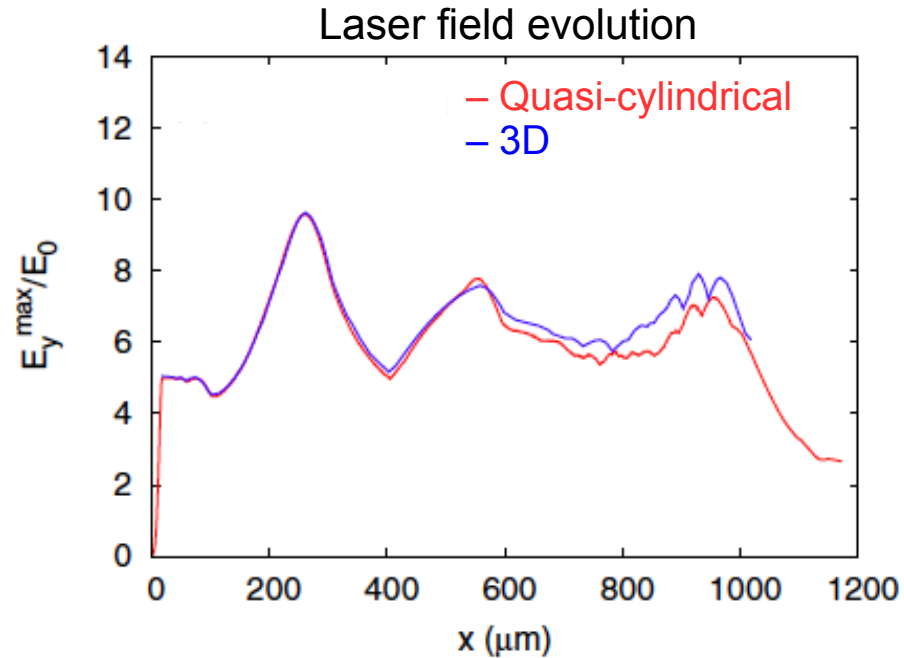
- equations for different azimuthal modes decouple (i.e., equations for  $m=0$  are solved independently from  $m=1$ , etc..)
- “standard” 2<sup>nd</sup> order\* or PSATD schemes are available

- Push particles

- equations for the numerical particles are solved in 3D Cartesian coordinates (requires reconstructing the fields in Cartesian geometry but avoids problems related to “singularity” in  $r=0$ )
- particle quiver in the laser field modeled (no averaged ponderomotive approx.)

# Quasi-cylindrical codes reproduce 3D physics at a $\sim 2D$ computational cost $\rightarrow$ large savings

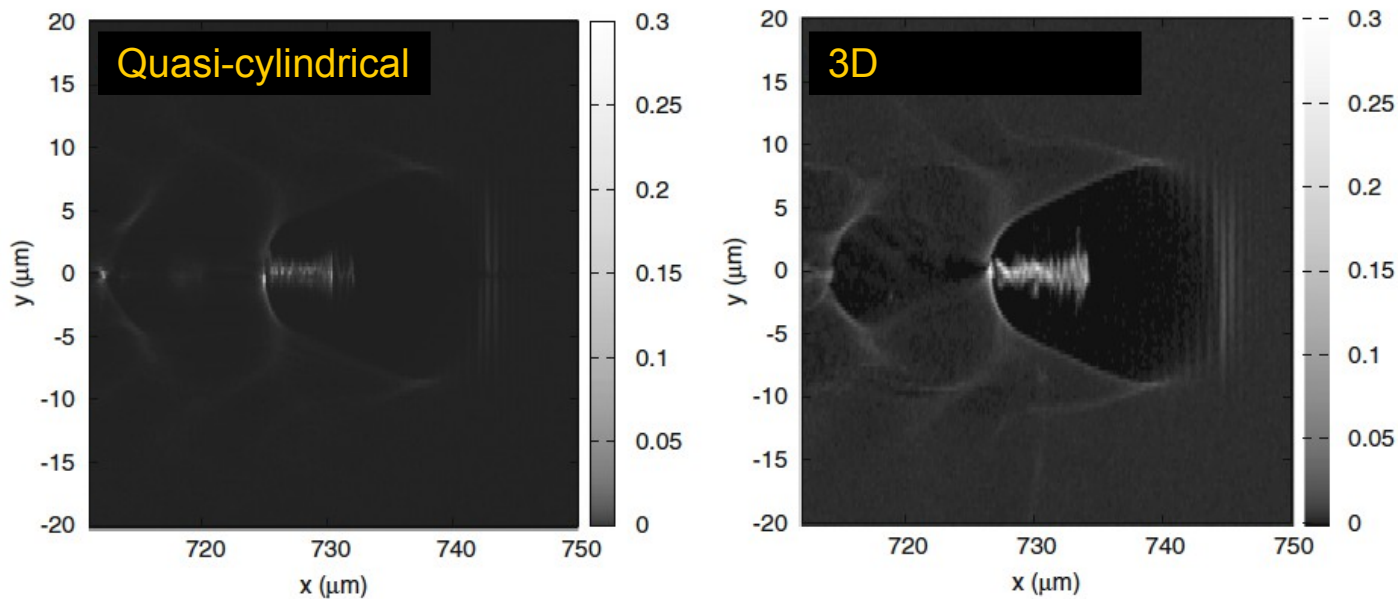
$a_0 = 5$   
 $T_0 = 30$  fs  
 $w_0 = 9$   $\mu\text{m}$   
 $n_0 = 1.2 \times 10^{19}$   $\text{cm}^{-3}$   
(uniform density)



Simulation with CALDER  
(CALDER-circ):

3D  $\rightarrow$  7000 CPUh  
Quasi-cylindrical  $\rightarrow$  70 CPUh

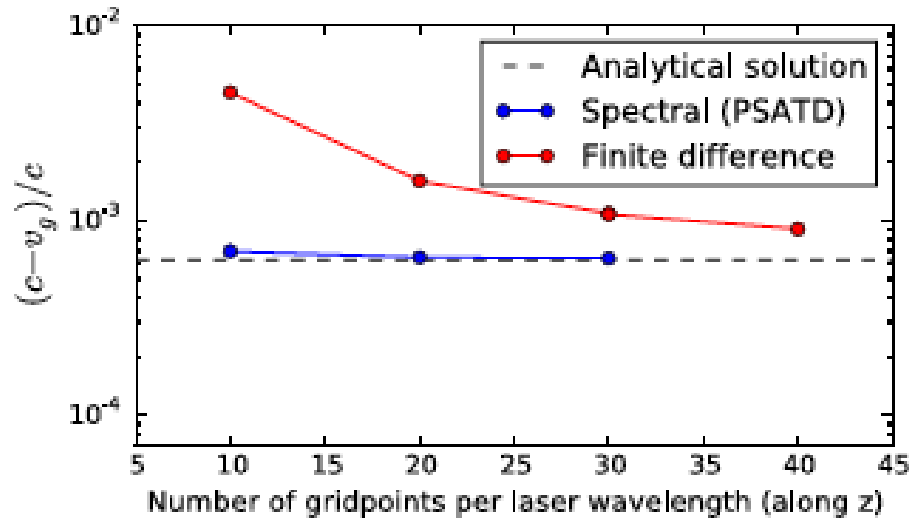
Electron density  $\rightarrow$



# Combining quasi-cylindrical + spectral (FBPIC)

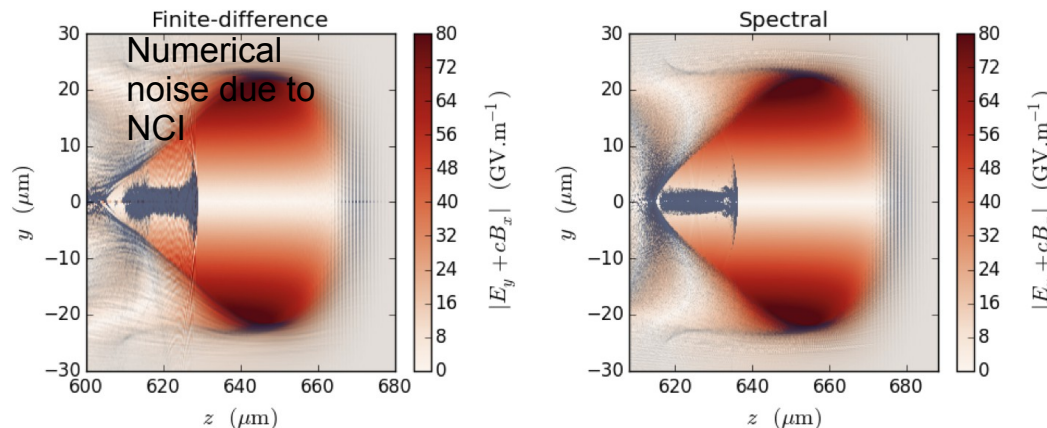
Advantages of a quasi-cylindrical modality (computational savings) combined with the advantages of a spectral field solver (superior description of EM waves propagation)

Correct laser group velocity →



Typical laser-wakefield simulation:

Suppression of NCI →



# References

## **Lorentz boosted frame:**

- J.-L. Vay, PRL 98, 130405 (2007)
- J.-L. Vay et al., Phys. Plasmas 18, 123103 (2011)

## **Mitigation of NCI in Lorentz boosted frame:**

- B. B. Godfrey and J. L. Vay, Computer Physics Communications 196, 221 (2015)
- P. Yu et al., Computer Physics Communications 192, 32 (2015)
- P. Yu et al., Computer Physics Communications 197, 144 (2015)
- R. Lehe et al., Phys Rev. E 2016, 053305 (2016)
- M. Kirchen et al., Phys. Plasmas 23, 100704 (2016)

## **Laser-envelope description:**

- C. Benedetti, et al., AIP Conference Proceedings 1299, 250 (2010)
- C. Benedetti, et al., AIP Conference Proceedings 1812, 050005 (2017)
- D. Gordon, IEEE Transactions on Plasma Science 35, 1486 (2007)
- B. M. Cowan, et al., J. Comp. Phys. 230, 61 (2011)

## **Quasi-static approximation:**

- P. Mora and T. Antonsen, Phys. Plasmas 4, 217 (1997)
- C. Huang al., Journal of Computational Physics 217, 658 (2006)
- W. An et al., Journal of Computational Physics 250, 165 (2013)
- T. Mehrling et al., Plasma Physics and Controlled Fusion 56, 084012 (2014)

## **Quasi-cylindrical:**

- A. F. Lifschitz et al., Journal of Computational Physics 228, 1803 (2009)
- A. Davidson et al., Journal of Computational Physics 281, 1063 (2015)
- R. Lehe et al., Computer Physics Communications 203, 66 (2016)